U. of Iowa 69-17

Distribution of this document is unlimited.

Department of Physics and Astronomy

THE UNIVERSITY OF IOWA

Iowa City, Iowa

The Correlation of Solar Microwave and Soft X-Ray Radiation

1. The Solar Cycle and Slowly Varying Components*

Charles D. Wende**

Department of Physics and Astronomy
The University of Iowa
Iowa City, Iowa 52240

March 1969

NGL-16-001-002

*This research was supported in part by the Office of Naval Research under contract Nonr 1509(06), by the National Aeronautics and Space Administration under grant NsG 233-62, by the Jet Propulsion Laboratory under contract JPL 951563, and by the Goddard Space Flight Center of the National Aeronautics and Space Administration under contract NAS5-9076.

**Now at National Space Science Data Center, Goddard Space Flight Center, Greenbelt, Maryland 20771

ABSTRACT

The integral solar x-ray flux between 2-12 A was measured by the spacecrafts Injun 1, Injun 3, Explorer 33, and Explorer 35. The integral flux between 2-9 A was observed by the Mariner V spacecraft. The data from Injuns 1 and 3 and Explorers 33 and 35, when averaged in monthly intervals, show a long term variation in activity of at least a factor of five between 1961 and 1969. A slowly varying component which tracks the 10 cm radio flux is observed in the x-ray flux. This x-ray flux variation, about a factor of ten, correlates with the appearance of major active regions on the solar disc. This slowly varying component correlates well with radio fluxes at frequencies greater than about 1 GHz and less well with radio fluxes at lower frequencies. The x-ray spectrum, obtained by comparing the 2-9 A flux with the 2-12 A flux, hardens during periods of high solar activity and may harden during flares, but does not soften.

I. INTRODUCTION

Solar radio emissions are often divided into three components. These are the quiet sun component, with a time scale of 11 years, the slowly varying component, with a time scale of about a month, and the burst component, with a time scale of seconds to hours. X-ray counterparts to these emissions have been found by Kundu [1963 and 1964], Friedman [1964], and Mandelshtam [1965]. The correlation between these two solar emissions will be studied in two papers, of which this, part 1, will deal with the quiet sun and slowly varying components. The second paper, part 2, will deal with the burst component.

II. SOFT X-RAY INSTRUMENTATION

The earliest University of Iowa solar x-ray observations were made by the satellite Injun 1 from 29 June 1961 through 12 August 1962 [Van Allen et al., 1965]. The next series of x-ray observations was made by the satellite Injun 3 during the period 30 December 1962 through 13 October 1963 [Wende, 1966]. A major improvement in the University of Iowa x-ray observations was made in the instrumentation of Explorer 33, which was launched on 1 July 1966 and is still operating as of the date of writing (March 1969). Whereas observations obtained with the Injun series of satellites were sporadically spaced in time, the Explorer 33 satellite provided essentially continuous observations [Van Allen, 1967]. Mariner V, operational from 14 June 1967 through 21 November 1967, provided continuous observations over a narrower wavelength range than Explorer 33 [Van Allen and Krimigis, 1968]. Explorer 35 [Van Allen and Ness, 1968], launched on 19 July 1967, has provided a continuing series of solar x-ray observations as well as in-flight determination of the angular corrections for the Explorer 33 observations, and is still operating as of the date of writing.

The soft x-ray sensors flown by the University of Iowa have been type 213 (Anton) or type 6213 (EON) Geiger tubes. These Geiger tubes have a mica window with a thickness of about 1.8 mg cm^{-2}. Only the Mariner V Geiger tube, however, was calibrated experimentally for soft x-ray use prior to launch. It had an additional 0.002 inch beryllium foil placed over the window and was calibrated both with and without the foil in place. The foil limited the long wavelength edge of the detector to about 9 A, rather than the 12 A limit of the unshielded Geiger tubes (see Table I).

III. CALIBRATION OF INSTRUMENTATION

The counting rate of a Geiger tube is given by

$$R = a \int \epsilon(\lambda)\, n(\lambda) d\lambda \ , \qquad (1)$$

where R = the counting rate in sec^{-1},

$\epsilon(\lambda)$ = the photon efficiency at wavelength λ, or the fraction of incident photons counted,

$n(\lambda)$ = the incident flux of photons, in $cm^{-2}\ sec^{-1}\ A^{-1}$,

a = the effective area of the Geiger tube in cm^2,

and it is assumed that the x-ray beam is perpendicular incident on the window of the Geiger tube. The efficiency is determined theoretically by the product of the window transmission, $T_w(\lambda)$, and the absorption of the filler gas, $A_g(\lambda)$. For a non-reflecting gas, the sum of the transmission, $T_g(\lambda)$, and the absorption, $A_g(\lambda)$, is unity. Thus,

$$\epsilon(\lambda) = T_w(\lambda)\ [1 - T_g(\lambda)] \ , \qquad (2)$$

where

$$T(\lambda) = \exp[-(\mu/\rho)\ \rho x] \ ,$$

(μ/ρ) = the mass absorption coefficient, and

ρx = the thickness of the window, w, or the gas, g, in $g\ cm^{-2}$. ([illegible])

The gas pressure of a sample of Geiger tubes from different batches from the manufacturer, as measured non-destructively via the inpop-outpop method of Van Allen [Van Allen et al., 1965], was 40.1 cm of Hg with extreme values of 59.5 and 17.0 cm of Hg. The gas absorption was calculated using the manufacturers specified filler gas of 440 mm of Hg of neon, 7.5 mm of Hg of argon, and 12.5 mm of Hg of chlorine. A path length, x, of 0.75 cm was used. The results of this calculation are shown in Fig. 1

The thickness of the mica window is about 1.8 mg cm^{-2}. Although the mica is believed to be muscovite, $Al_3\ (Si\ O_4)_3\ KH_2$, natural mica is often found in admixtures with various mica subspecies [Clarke, 1914]. A further problem arises in that the mass absorption coefficients for potassium, K, and silicon, Si, are not tabulated in the wavelength region of interest. For wavelengths shorter than the K absorption edge, λ_k, calculations have been made [Victoreen, 1949]. Unfortunately, the K edges of K and Si fall between 1 and 15 A. Since the slope of (μ/ρ) versus λ is about the same for wavelengths shorter and longer than λ_k, if the magnitude of the discontinuity at λ_k in (μ/ρ) can be found, complete values of (μ/ρ) can be extrapolated. Plotting (μ/ρ) as a function of λ for materials of atomic numbers near those of potassium (19) and silicon (14) yields Fig. 2. From this figure the discontinuity was estimated, and values of (μ/ρ) were extrapolated (the dotted lines) and were used to calculate window transmissions for various mica subspecies (see Fig. 3). The effect of using micas other than muscovite was generally to decrease the window transmission, particularly at the longer wavelengths.

The efficiency was measured experimentally by comparing the counting rate of a 6213 Geiger tube with the counting rate of a standard tube when both traversed a monochromatic beam. The standard tube was an EON 6251, which had a beryllium window and an argon filler gas. The window was masked so that only a portion of the gas free of obstruction (i.e., the central anode wire) interacted with the x-ray beam. The efficiency of the standard Geiger tube was calculated. The monochromatic x-ray beam was produced by a Bragg spectrometer used as a monochromator. A beam of soft x rays was generated by a cathode-anode x-ray tube (tungsten filament--tungsten target) operated in a vacuum. The cathode-anode potential and the cathode current could be varied independently. The x-ray beam passed through a collimator made of iron shim stock (Soller slit). The collimated beam was then diffracted by a crystal and Bragg's law,

$$n\lambda = 2d \sin \theta , \qquad (4)$$

where n = the order of the diffraction

λ = the wavelength of the diffracted beam,

d = the spacing between the layers of the crystal, and

θ = the angle between the incident beam and the surface of the crystal,

was assumed. Two crystals were used, potassium acid phthalate (KAP, d = 13.3 A) and ammonium dihydrogen phosphate (ADP, d = 5.3 A). By maintaining the lowest usable anode-cathode potential, second and higher order Bragg diffraction was eliminated as the wavelengths responsible did not appear in the beam incident upon the crystal. The two Geiger tubes were moved across the diffracted beam (e.g., see Fig. 4), and the ratio of the counting rates due to the x-ray beam yielded the efficiency of the 6213 from

$$\beta(\lambda) = \frac{\epsilon'(\lambda)\ a'\ n'(\lambda)\Delta\lambda}{\epsilon(\lambda)\ a\ n(\lambda)\Delta\lambda}\ , \qquad (5)$$

where $\beta(\lambda)$ = the ratio of the counting rates,

$\epsilon'(\lambda)$ = the photon efficiency of the 6213,

$\epsilon(\lambda)$ = the photon efficiency of the standard tube,

a' = the effective area of the 6213,

a = the effective area of the standard tube, about $1.1\ a'$,

$n'(\lambda)\Delta\lambda$ = the photon flux incident upon the 6213, and

$n(\lambda)\Delta\lambda$ = the photon flux incident upon the standard tube.

Since the photon fluxes were the same, the ratio of the counting rates yielded the ratio of the efficiencies at the wavelength λ.

The results of the experimental calibration (without the beryllium foil in place) are presented in Fig. 5. The solid line represents the theoretical efficiency for a Geiger tube with a gas of 440 mm of Hg of neon, 7.5 mm of Hg of argon, and 12.5 mm of Hg of chlorine with an effective path length of 0.75 cm behind a window of pure muscovite mica 1.8 mg cm^{-2} thick. The discrepancy in the efficiency at the K edge of aluminum may be due to the presence of sericite in the mica. The calculated and experimentally determined efficiencies agree to within the known uncertainties in the construction and filling of the Geiger tube.

The conversion factor, γ, relating the counting rate, R, in counts sec^{-1}, to the energy flux in a specified wavelength range, in ergs cm^{-2} $count^{-1}$, is given by

$$\gamma = \frac{F(0 - \lambda)}{R} = \frac{\int_0^{\lambda} F(\lambda')\, d\lambda'}{a \int \epsilon(\lambda') n(\lambda') d\lambda'} , \qquad (6)$$

where $F(0 - \lambda)$ = the energy flux in the 0 to λ A range in ergs cm^{-2} sec^{-1},

$F(\lambda')$ = the differential energy flux incident upon the Geiger tube, in ergs cm^{-2} sec^{-1} A^{-1},

a = the effective area of the Geiger tube,

$\epsilon(\lambda')$ = the photon efficiency of the Geiger tube at wavelength λ', and

$n(\lambda')$ = the differential photon flux incident upon the Geiger tube, or $F(\lambda')/h\nu'$, where $h\nu'$ is the photon energy.

The factor γ determined for Explorer 33 and also applicable to Explorer 35 was 1.8×10^{-6} ergs cm^{-2} sec^{-1} over the wavelength range from 2 to 12 A [Van Allen, 1967]. The determination of γ for Mariner V is illustrated in Fig. 6. The distribution in the values of γ as a function of λ form a bow-tie, and γ was chosen to fall in the knot of the tie, where the differences in γ due to different spectra (i.e., black body, free-free, or a spectrum softer than free-free by a factor of $(1/\lambda^2)$) are minimized. The wavelength at which this knot occurs determines the effective long wavelength edge of the detector. For Mariner V, γ was chosen as 3.5×10^{-6} ergs cm^{-2} $count^{-1}$ over a wavelength interval of 2 to 9 A. The short wavelength limit is the same as that of Van Allen [1967], since the beryllium foil has little effect at short wavelengths.

IV. THE SOLAR CYCLE VARIATION AND THE QUIET SUN COMPONENT

The overall level of solar activity, as indicated by sunspot numbers or radio flux indices, varies over an eleven-year period. This variation reflects the number and size of active regions, such as sunspots or plage, existing on the sun at any given time. To examine this variation, it is useful to use monthly time blocks as they correspond to the approximate period of one solar rotation. Thus, if one averages x-ray or radio fluxes in monthly intervals one has an average flux indicative of the level of activity on the entire sun and not just indicative of the activity on the visible disc. In this spirit, Fig. 7 illustrates observed soft x-ray fluxes and 10 cm radio fluxes averaged in monthly intervals. In both cases flare data were deleted. The fluxes observed by Injun 1 and Explorers 33 and 35 are about an order of magnitude higher than the fluxes observed by Injun 3. The maximum variation in counting rate between any two of the four Geiger tubes flown on Explorers 33 and 35 was less than a factor of 2 prior to normalization. Thus the observed variation in the x-ray flux must be at least a factor of 5 and is not instrumental. Over the same period, the 10 cm radio flux varied by about a factor of 2. The times of the minimum x-ray and radio flux levels agree (i.e., the summer of 1963) and, hence, a solar cycle variation in the soft x-ray is strongly suggested.

The quiet sun component is defined as "the emission of the solar atmosphere when the contributions from all discrete sources of the slowly varying component are subtracted [Kundu, 1964]." Although the quiet sun component has been studied statistically at radio wavelengths [Pawsey and Yabsley, 1949], the data obtained from Injun 3 were not of a nature to permit such a statistical analysis. However, the minimum x-ray flux observed by either Explorer 33 or Explorer 35 was 0.39 milliergs cm^{-2} sec^{-1}. This minimum flux is greater than some of the average fluxes observed by Injun 3 and suggests the presence of a quiet sun component. The quiet sun component has been observed at soft x-ray wavelenghts by others [Mandelshtam, 1965; Friedman, 1964].

V. THE TEMPORAL VARIATION DUE TO THE SLOWLY VARYING COMPONENT

Figure 8 illustrates the temporal variation in the x-ray flux observed by Mariner V. The non-flare flux observed on each day at about 1650 G.M.T. was used as this flux value could be correlated with non-flare radio fluxes measured at 1640 G.M.T. by the AFCRL and at 1700 G.M.T. at Ottawa.

Periods of enhanced activity are evident during the latter halves of solar rotations 1833, 1834, and 1836.

The enhancement of activity beginning around 20 July was due to a series of active regions which were rotated onto the northeast limb beginning on 21 July (Preliminary Report of Solar Activity, 1967). The most important active region was a large and complex spot group located at N27 W02 on 28 July (McMath plage number 8905) which completed its west limb passage on 4 August.

The enhancement of activity centering about 25 August was due primarily to an active region located at N22 which had its meridian passage on 25 August (Preliminary Report of Solar Activity, 1967). This region, McMath plage number 8942, is believed to be the reappearance of plage number 8905. It grew both in plage and sunspot area after its east limb passage, began to decay on 24 August, and passed the west limb on 1 September.

The enhancement of activity centering about 28 October was due to an active region located at N10, McMath plage number 9034. This region was developing features characteristic of a major active region as it passed the west limb on 29-30 October (Preliminary Report of Solar Activity, 1967).

The x-ray flux clearly tracks the slowly varying component observed at 10 cm. The discrepancy between the x-ray flux levels and the terrestrially observed radio fluxes measured in late October in probably due to the effect of the earth-sun-Mariner angle, which was about 40 degrees at that time. Thus, the Mariner instrumentation could observe a solar phenomenon three days after it had disappeared behind the west limb when viewed from the earth. Prior to 30 August, the earth-sun-Mariner angle was less than 5 degrees, and by 30 September it was still only 15 degrees.

The daily x-ray flux observed in the fall of 1967 is illustrated in Fig. 9. On physical grounds, the flux in the 2-12 A band must be greater than the flux in the 2-9 A band. In late October and early November this condition does not necessarily occur. This variance is believed to indicate that the Mariner detector observed emissions not observed by Explorer 35 which, although it is a lunar orbiter, in this case can be considered a terrestrial observer.

From the time that it takes for a source to disappear from view, the height of the emitting region can be estimated assuming that the photosphere is optically thick at the observing wavelength and that the chromosphere and corona are optically thin. It is necessary that the source being observed is stable so that one is certain that the disappearance behind the limb, and not the decay of the source, is being observed. The disappearance of plage 9034 was observed by Explorer 35 as the Mariner observations showed that the plage was not decaying. If plage 8942 was truly the return of plage 8905, then it can be assumed that the disappearance of plage 8905 was observed. There is no evidence that the decrease in the x-ray flux around 1 September was due solely to the disappearance of plage 8942 and not in part to its decay, which had been observed to start on 24 August.

As it took approximately two days for the fluxes associated with plage 8905 and with plage 9034 to decrease to one half their pre-limb passage value, the apparent heights of the active regions, as observed in the soft x-ray radiation, are 6.8×10^4 km for plage 8905 and 7.6×10^4 km for plage 9034.

VI. THE CORRELATION OF THE SLOWLY VARYING COMPONENT AT RADIO AND SOFT X-RAY WAVELENGTHS

From Fig. 8 it is apparent that the non-flare soft x-ray flux correlates well with the 10 cm non-flare radio flux. Scatter plots illustrating the correlation between the 2-9 A x-ray flux observed by Mariner V and various radio flux indices are shown on Fig. 10. The correlation is somewhat better at frequencies of 2800 MHz and 8800 MHz when compared with the correlation observed at 225 MHz as at 225 MHz one observes low radio fluxes during periods of high x-ray fluxes. At the higher frequencies, one always observes relatively high radio fluxes during periods of high x-ray fluxes.

Assuming a linear correlation (i.e., the x-ray flux was assumed proportional to the radio flux), correlation coefficients were determined which characterized the correlation between the 2-9 A x-ray flux and the radio flux at various frequencies (see Fig. 11). The radio fluxes used were the 2800 MHz flux obtained at Ottawa, the 8800 MHz, 4995 MHz, 2695 MHz, 1415 MHz, and 606 MHz flux measured at the Sagamore Hill Observatory, and the 225 MHz flux measured at the Oslo Solar Observatory as listed either in the bulletin Solar Geophysical Data (1967) or the Geophysics and

Space Data Bulletin (1967). The x-ray data were taken prior to 10 September 1967, when the earth-sun-Mariner angle was less than 9 degrees. The correlation coefficients are somewhat higher for frequencies greater than about 1 GHz than are the coefficients obtained using the lower two frequencies.

These coefficients can be compared to the correlation coefficients obtained using 2-12 A x-ray fluxes [Wende, 1966] and extreme ultraviolet between 10-100 A [Kundu, 1963]. These coefficients are illustrated in Fig. 12. The 10-100 A flux was measured by Kundu indirectly through the use of an E-layer ionospheric index, ($f_oE^4/\cos Z$). The correlation obtained was quite good if frequencies higher than about 1 GHz were used, but decreased sharply when frequencies below 1 GHz were used. The 2-12 A flux was obtained from two type 213 Geiger tubes flown on Injun 3. These two Geiger tubes, labelled 213-130 and 213-90, were treated independently as they were not calibrated for soft x-ray use prior to launch. The correlation coefficients obtained using the 213-130 tended to reflect the results of Kundu obtained in the 10-100 A band, while the coefficients obtained using the 213-90 reflected the results of the Mariner data in the 2-9 A band. The discrepancy between the results using the 213-90 and the 213-130 is believed due to the different observing periods of the two detectors, the 213-90 observations having been made during a period of much lower solar activity (late June, July, and early August of 1963) than the 213-130 observations (May and early June, 1963). This discrepancy was taken to indicate that radio fluxes at frequencies below about 1 GHz are less reliable indicators of soft x-ray fluxes than radio fluxes at higher frequencies.

In view of the low 225 MHz fluxes observed during periods of high soft x-ray fluxes and the results from the Injun 3 data mentioned above, it is felt that radio fluxes observed at frequencies higher than about 1 GHz are consistently good indicators of x-ray fluxes in the 2-9 A and 2-12 A bands and even in the 10-100 A band [from Kundu, 1963], whereas radio fluxes observed at frequencies below about 1 GHz are less reliable indicators of x-ray fluxes in the above bands.

VII. THE SPECTRAL VARIATION OF THE SLOWLY VARYING COMPONENT

By comparing the x-ray flux observed by Mariner V (2-9 A) with the x-ray flux observed by Explorer 35 (2-12 A), some spectral information can be gained. An example is Fig. 13, which illustrates the 2-9 A flux as a function of the 2-12 A flux observed simultaneously. One-hour averages of the data were taken every four hours commencing on 27 July 1967 and ending on 10 September. During this period 95 percent of the solar disc was viewed in common by both spacecraft. Points which included Explorer 35 data taken during eclipse were deleted, and points which included x-ray flares with a peak flux to background flux ratio of three or greater were indicated by an "X".

Two results are apparent from Fig. 13. First, during a flare the spectrum may harden, but does not soften. Secondly, during periods of high solar activity the spectrum is slightly harder than that observed during periods of low solar activity.

Since soft x-ray flares are believed generated by quasi-thermal bremsstrahlung released by electrons heated by the flaring process [De Jager, 1965], the spectrum would be expected to harden during flares. Further, as the slowly varying component is generated by abnormally hot regions in the solar atmosphere, the x-ray plage first observed by Friedman [1964], it would be expected that the spectrum would harden during periods of higher solar activity.

TABLE I. University of Iowa Soft X-Ray Observations

Spacecraft	Passband (Angstroms)	Interval between Samples	Duration of Samples	Operating Period
Injun 1	2-12	Sporadic	1^m	29 June 1961 to 12 August 1962
Injun 3	2-12	Sporadic	1^m	20 December 1962 to 13 October 1963
Explorer 33	2-12	82^s or 164^s	6.4^s over 26^s	1 July 1966 to present (March 1969)
Mariner V	2-9	101^s or 403^s	9.3 or 37.2^s	14 June 1967 to 21 November 1967
Explorer 35	2-12	82^s	6.4^s over 26^s	19 July 1967 to present (March 1969)

ACKNOWLEDGEMENTS

This research was submitted in partial fulfillment of the requirements for the degree of Doctor of Philosophy at The University of Iowa, Iowa City, Iowa. The author is grateful to Prof. J. A. Van Allen for his guidance and support of this work. Thanks are also in order for Profs. S. M. Krimigis and G. Payne for their informative discussions and interest in this project.

This research was supported in part by the Office of Naval Research under contract Nonr 1509(06), by the National Aeronautics and Space Administration under contract NsG 233-62, by the Jet Propulsion Laboratory under contract JPL 951563, and by the Goddard Space Flight Center of the National Aeronautics and Space Administration under contract NAS5-9076. The author was a National Aeronautics and Space Administration trainee during part of the time this work was in progress.

REFERENCES

Clarke, F. W., Constitution of Natural Silicates, p. 51, U. S. Government Printing Office, Washington, D. C., 1914.

De Jager, C., Solar x radiation, Ann. Astrophys., 28, 125, 1965.

Friedman, H., Ionospheric constitution and solar control, in Research in Geophysics, edited by H. Odishaw, Vol. 1, p. 157, M. I. T. Press, Cambridge, Mass., 1964.

Geophysics and Space Data Bulletin, IV, 3 and 4, edited by A. L. Carrigan and N. J. Oliver, Clearinghouse, Dept. of Commerce, Washington, D. C., 1967.

Kundu, M. R., Centimeter-wave radio and x-ray emission from the sun, Space Sci. Rev., 2, 438, 1963.

Kundu, M. R., Solar Radio Astronomy, University of Michigan Radio Observatory report No. 64-4, Ann Arbor, Mich., 1964.

Mandelshtam, S. L., X-ray emission of the sun, Space Sci. Rev., 4, 587, 1965.

Pawsey, J. L. and D. E. Yabsley, Solar radio-frequency radiation of thermal origin, Aust. J. Sci. Res., A, 2, 198, 1949.

Preliminary Report and Forecast of Solar-Geophysical Activity, Boulder, Colorado, TR No. 822-842, 1967.

Solar-Geophysical Data, ESSA Research Laboratories, IER-FB-275 through IER-FB-284, U. S. Government Printing Office, Washington, D. C., 1967.

Van Allen, J. A., L. A. Frank, B. Maehlum, and L. W. Acton, Solar x-ray observations by Injun I, J. Geophys. Res., 70, 1639, 1965.

Van Allen, J. A., The solar x-ray flare of July 7, 1966, J. Geophys. Res., 72, 5903, 1967.

Van Allen, J. A. and S. M. Krimigis, Preliminary Report on Magnetospheric, Solar, and Interplanetary Observations with Mariner V, University of Iowa report No. 67-58, Iowa City, Iowa, 1967.

Victoreen, J. A., The calculation of x-ray mass absorption coefficients, J. Appl. Phys., 20, 1141, 1949.

Wende, C. D., Solar X-Ray Observations by the Satellites Injun I and Injun III, unpublished Master's thesis, University of Iowa, Iowa City, Iowa, 1966.

FIGURE CAPTIONS

Figure 1. The calculated x-ray absorption of the filler gas in a 6213 Geiger tube.

Figure 2. The graphical extrapolation of μ/ρ for K and Si.

Figure 3. The window transmission of various micas 1.8 mg cm^{-2} thick.

Figure 4. A typical scan of a monochromatic x-ray beam.

Figure 5. The efficiency of a 6213 Geiger tube.

Figure 6. The determination of the effective bandpass and the corresponding conversion factor γ for Mariner V.

Figure 7. The solar cycle variation observed in the x-ray and radio flux. The fluxes are averaged in monthly intervals.

Figure 8. The history of Mariner V x-ray fluxes and 10 cm radio fluxes observed in 1967.

Figure 9. Mariner V and Explorer 35 x-ray fluxes observed in the fall of 1967.

Figure 10. Radio fluxes as a function of 2-9 A x-ray fluxes.

Figure 11. The correlation between 2-9 A solar x-ray fluxes and solar radio fluxes.

Figure 12. The correlation between solar x-ray and extreme ultraviolet fluxes and solar radio fluxes.

Figure 13. Observed 2-9 A and 2-12 A x-ray fluxes.

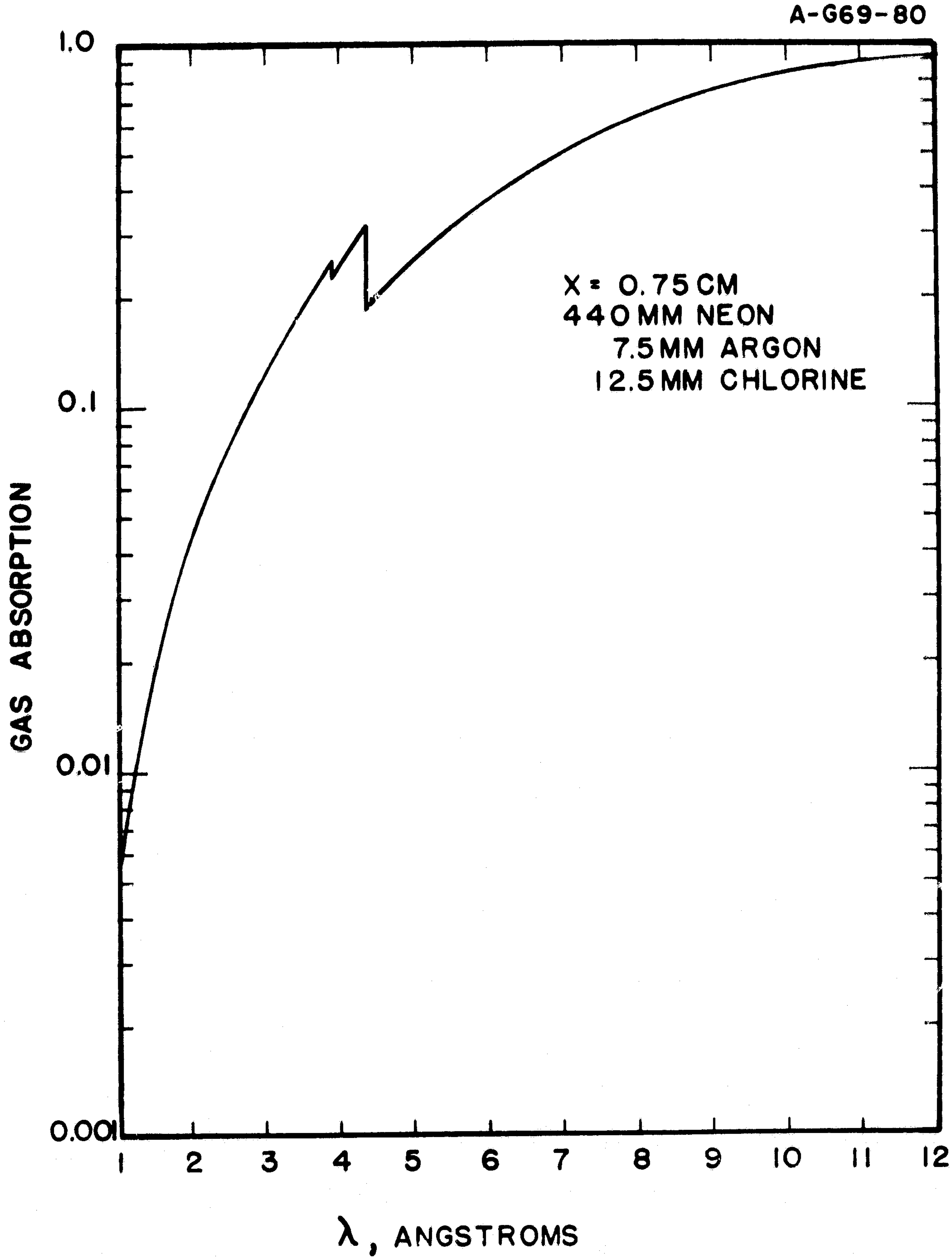
A-G69-80
1.0
0.1
0.01
0.001
GAS ABSORPTION
X = 0.75 CM
440 MM NEON
7.5 MM ARGON
12.5 MM CHLORINE
1
2
3
4
5
6
7
8
9
10
11
12
λ, ANGSTROMS

Figure 1

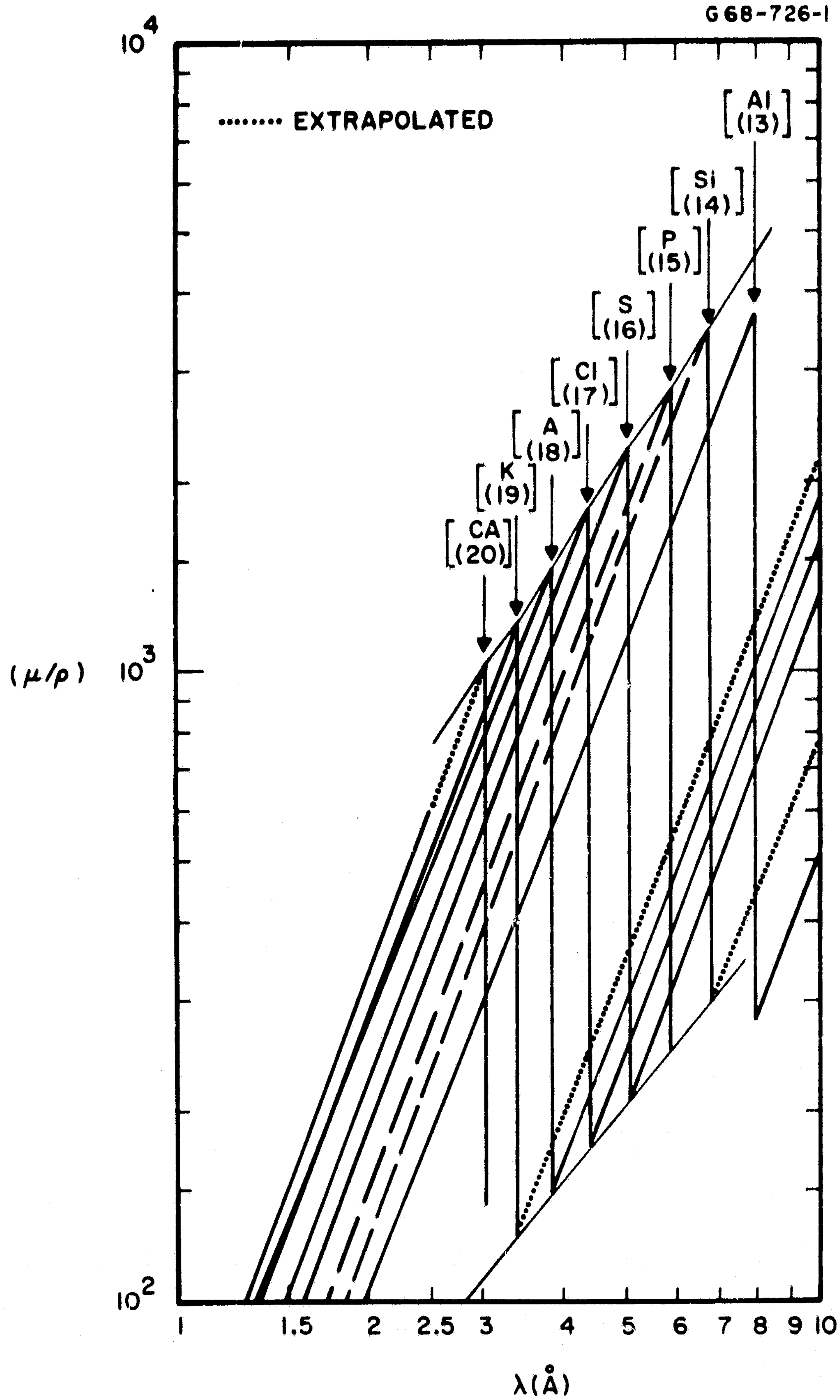
G68-726-1
EXTRAPOLATED
[Al (13)]
[Si (14)]
[P (15)]
[S (16)]
[Cl (17)]
[A (18)]
[K (19)]
[CA (20)]
10^4
10^3
10^2
(μ/ρ)
1
1.5
2
2.5
3
4
5
6
7
8
9
10
λ(Å)

Figure 2

G 68-728-1

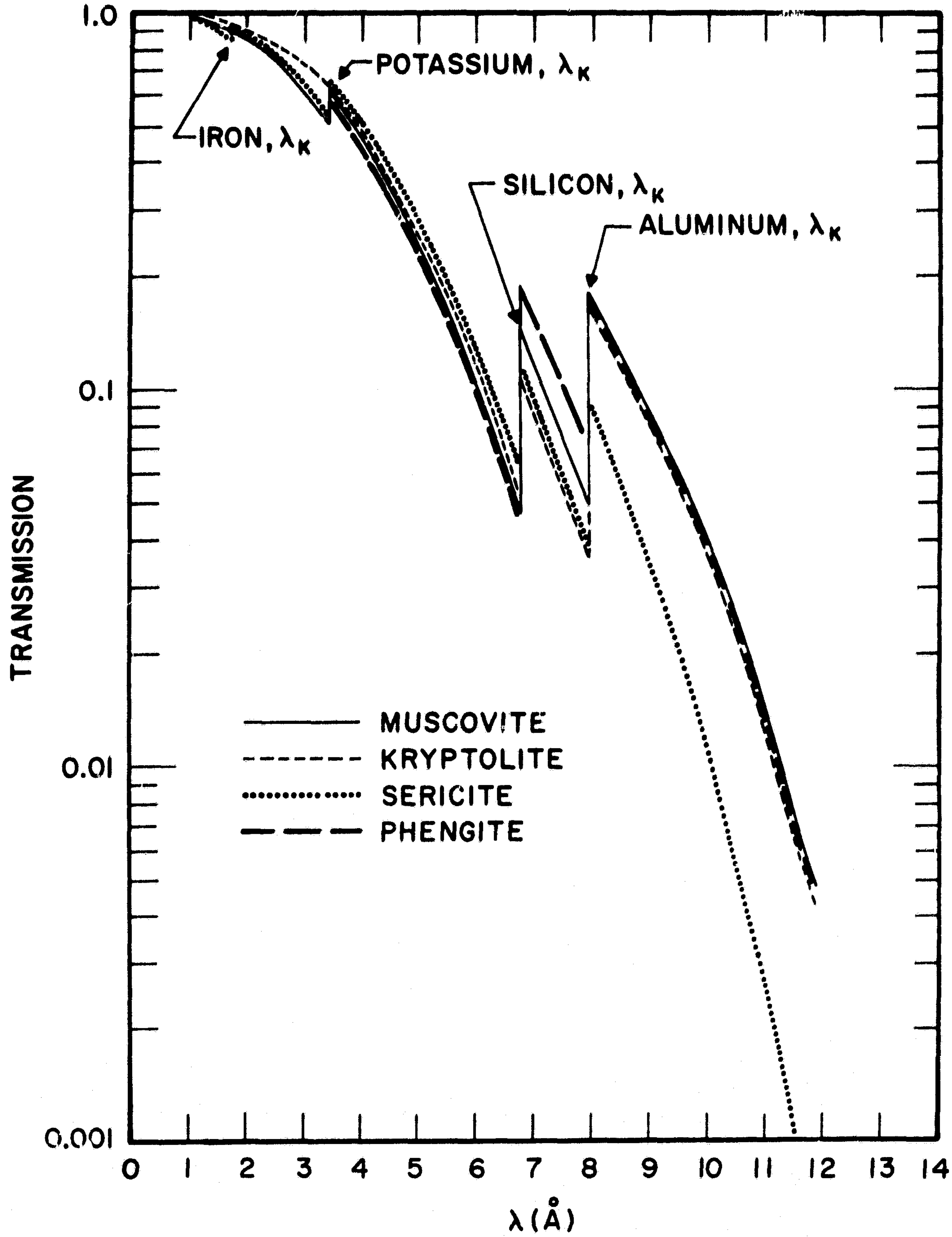

Figure 3

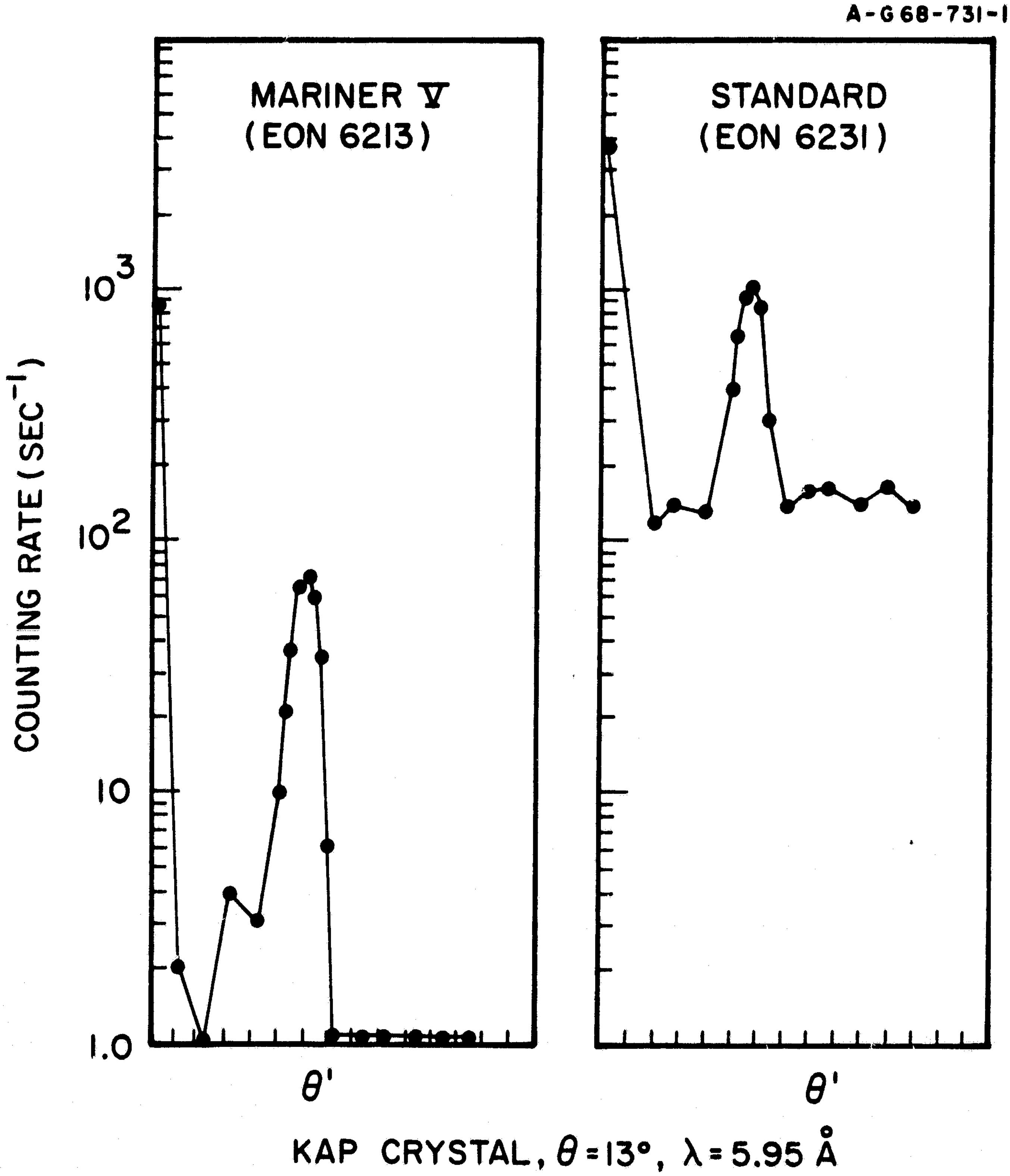
A-G68-731-1
MARINER V
(EON 6213)
STANDARD
(EON 6231)
COUNTING RATE (SEC^{-1})
10^3
10^2
10
1.0
θ'
θ'
KAP CRYSTAL, θ = 13°, λ = 5.95 Å

Figure 4

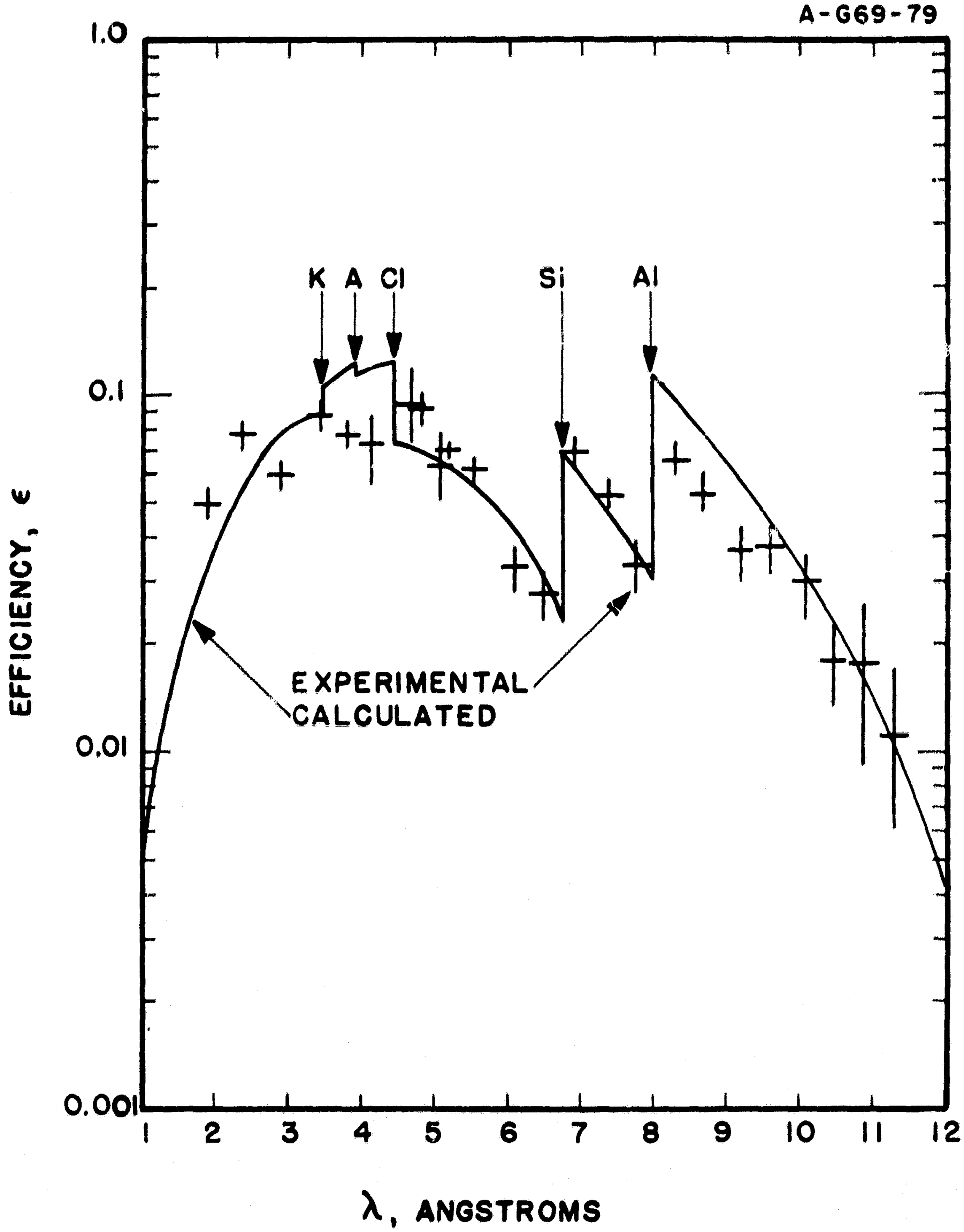
A-G69-79
1.0
0.1
0.01
0.001
EFFICIENCY, ε
K
A
Cl
Si
Al
EXPERIMENTAL
CALCULATED
1
2
3
4
5
6
7
8
9
10
11
12
λ, ANGSTROMS

Figure 5

068-721-1

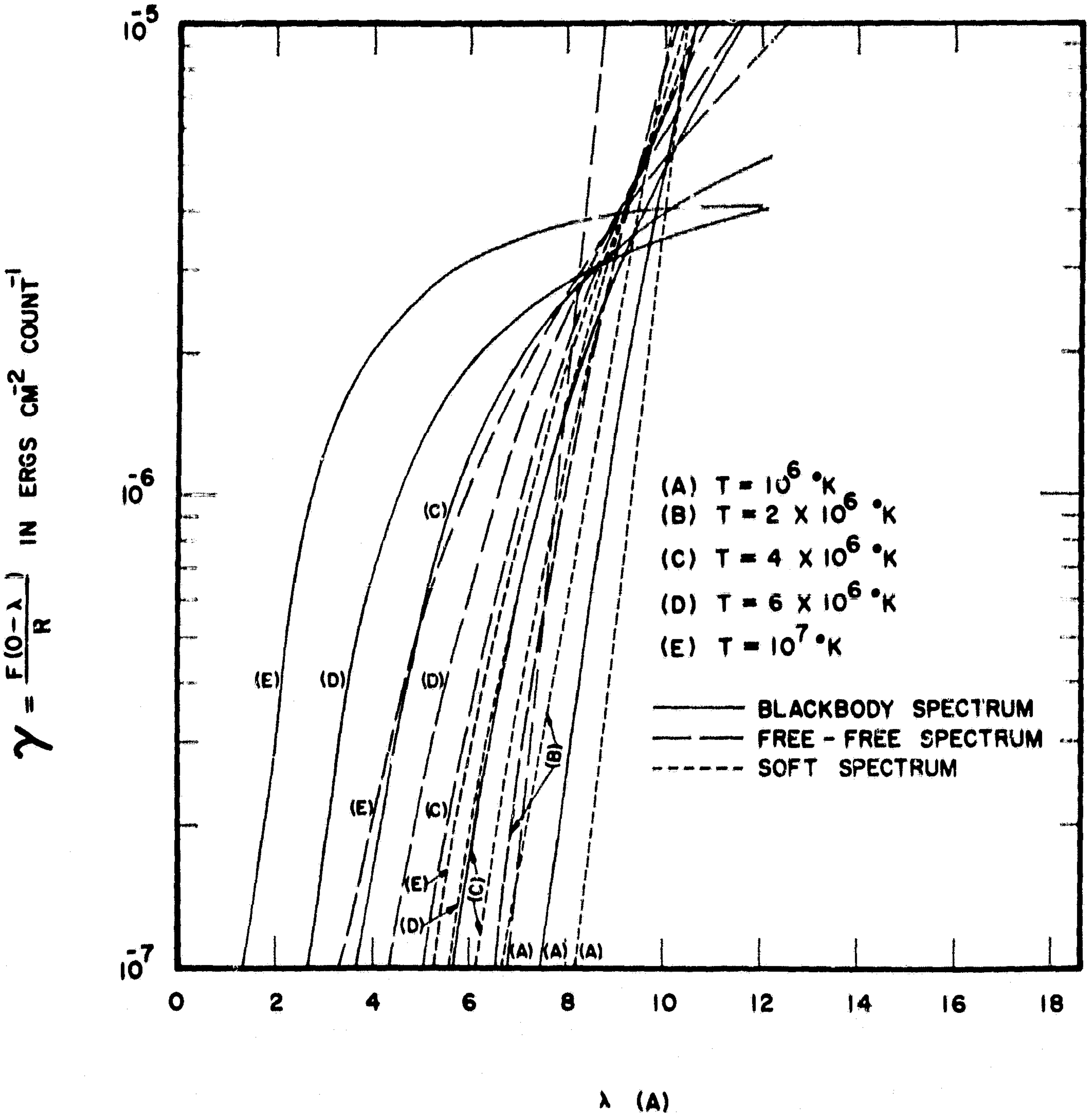

Figure 6

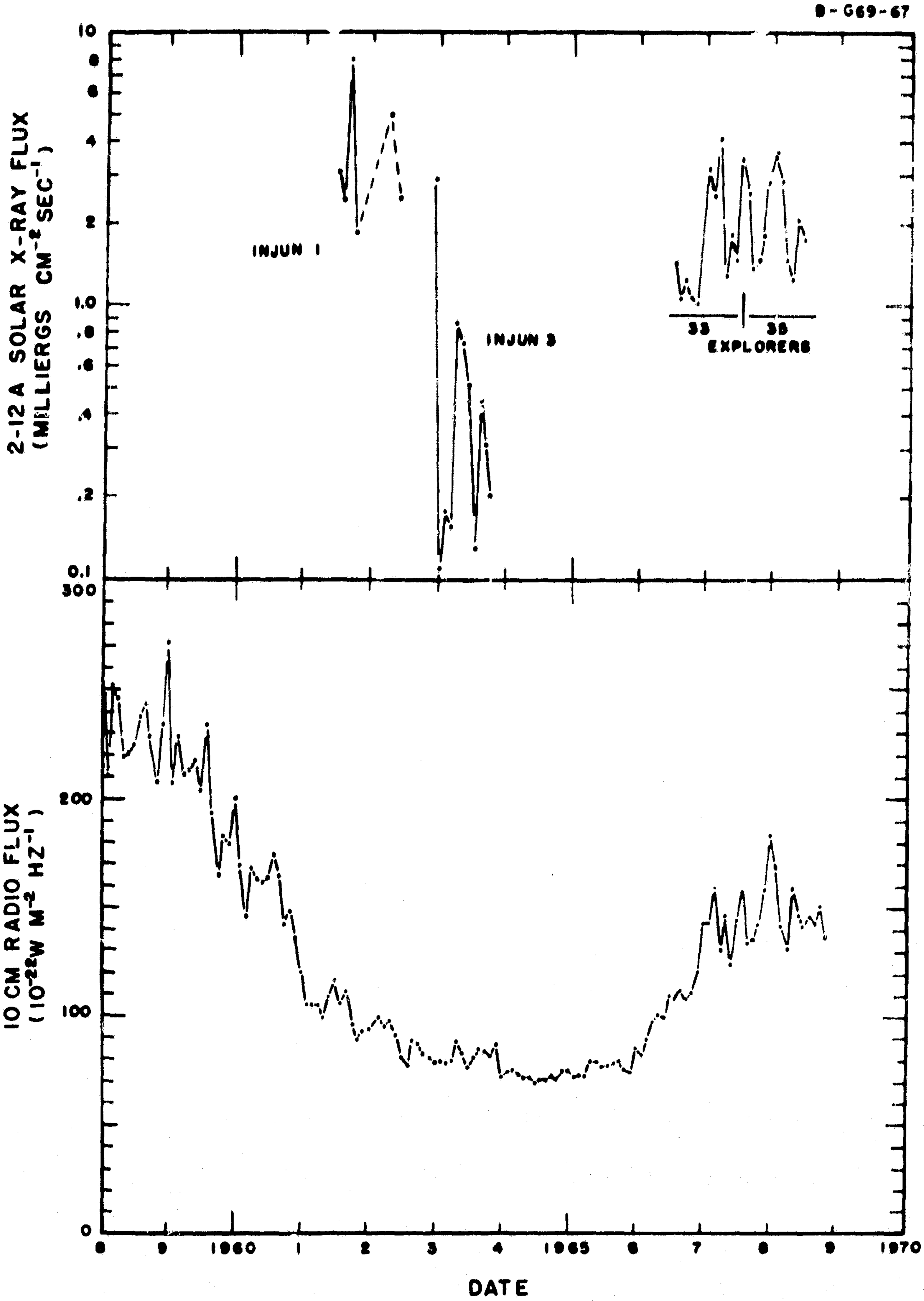
B-G69-67
2-12 A SOLAR X-RAY FLUX (MILLIERGS CM^{-2} SEC^{-1})
10
8
6
4
2
1.0
.8
.6
.4
.2
0.1
INJUN 1
INJUN 3
33
35
EXPLORERS
10 CM RADIO FLUX (10^{-22}W M^{-2} HZ^{-1})
300
200
100
0
8
9
1960
1
2
3
4
1965
6
7
8
9
1970
DATE

Figure 7

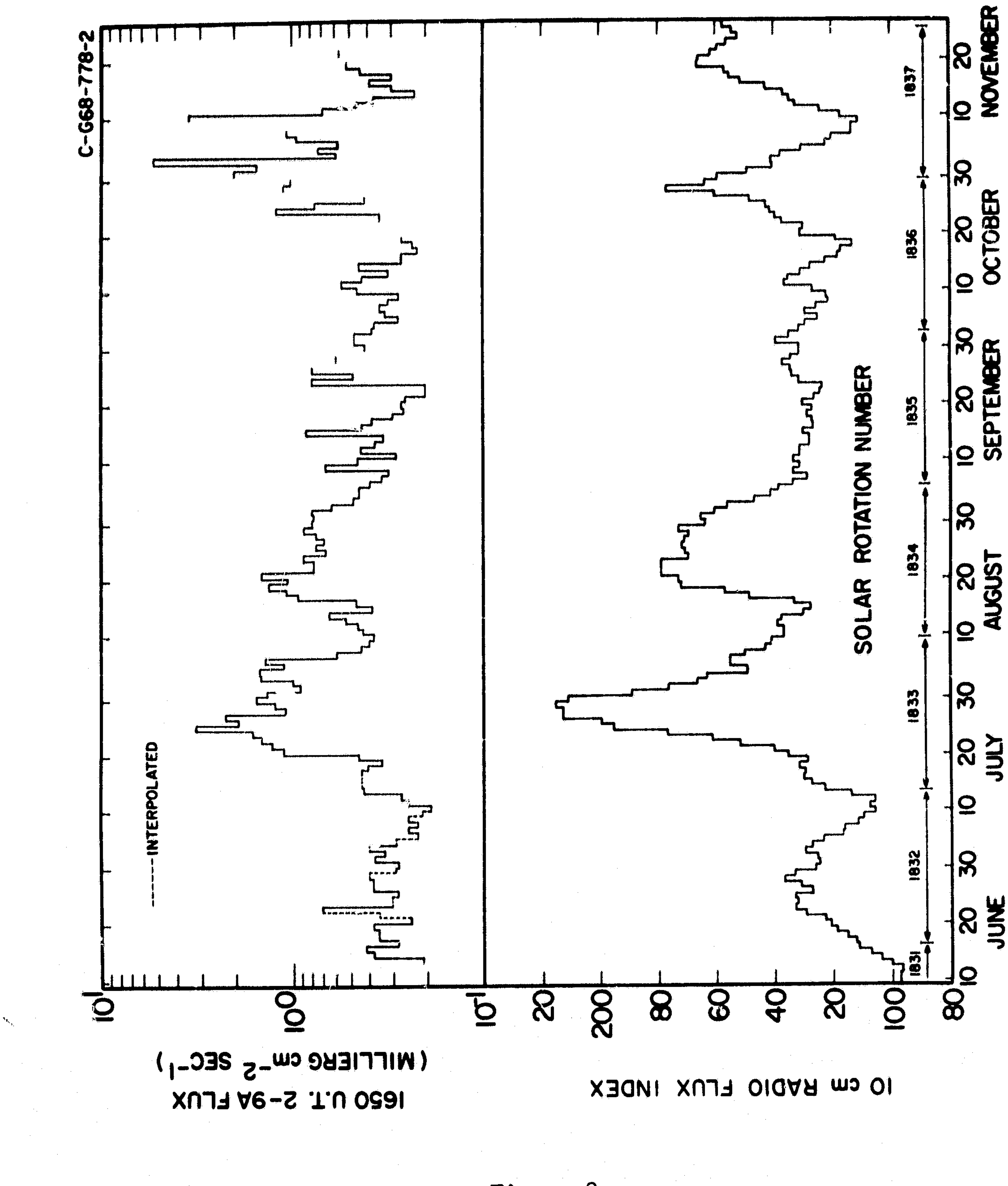

C-G68-778-2
INTERPOLATED
1650 U.T. 2-9A FLUX
(MILLIERG cm-2 SEC-1)
10 cm RADIO FLUX INDEX
SOLAR ROTATION NUMBER
1831
1832
1833
1834
1835
1836
1837
JUNE
JULY
AUGUST
SEPTEMBER
OCTOBER
NOVEMBER

Figure 8

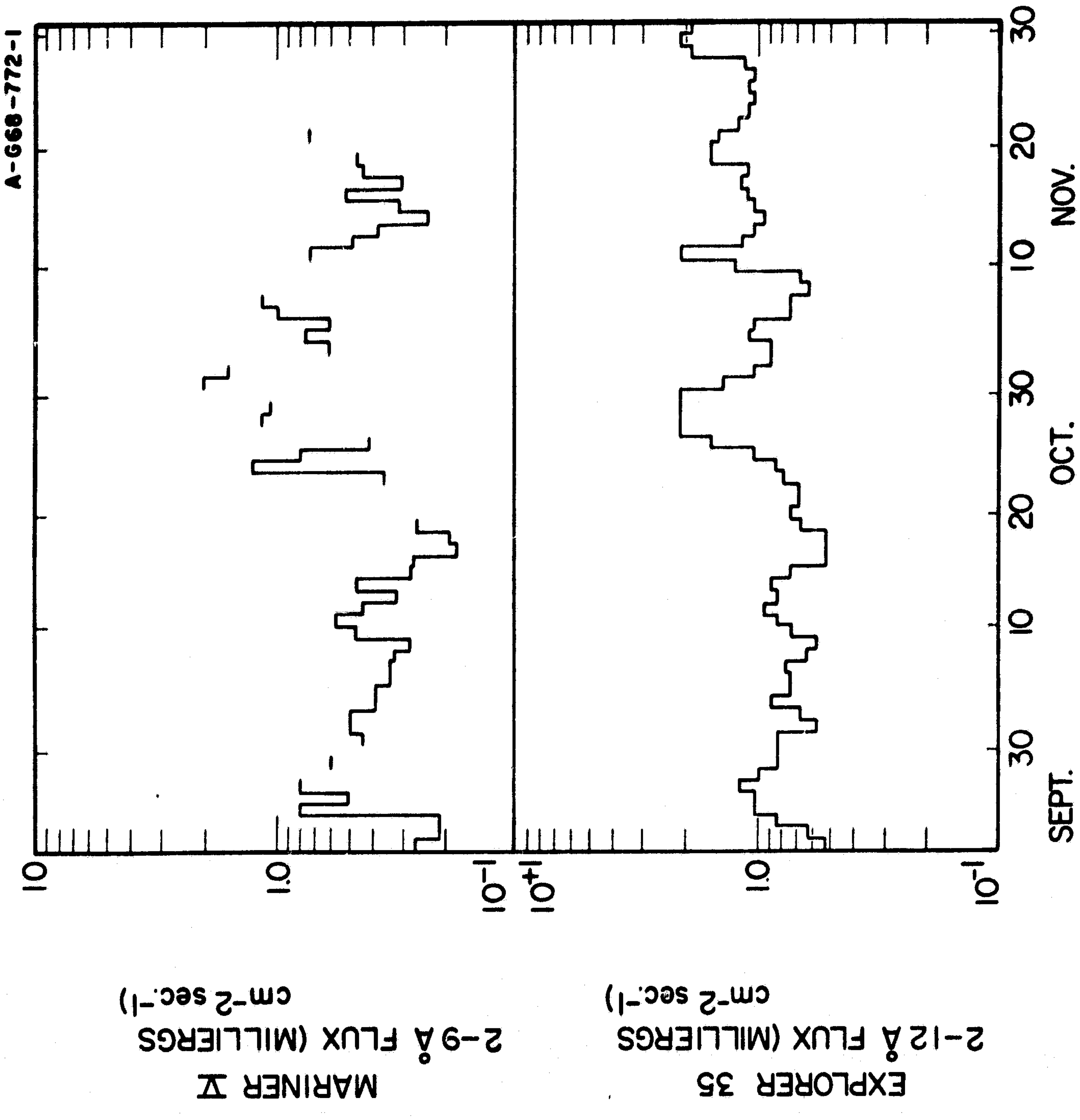
A-G68-772-1
MARINER V
2-9 Å FLUX (MILLIERGS
cm-2 sec.-1)
EXPLORER 35
2-12 Å FLUX (MILLIERGS
cm-2 sec.-1)
10
1.0
10-1
10+1
SEPT.
OCT.
NOV.
30
10
20
30
10
20
30

Figure 9

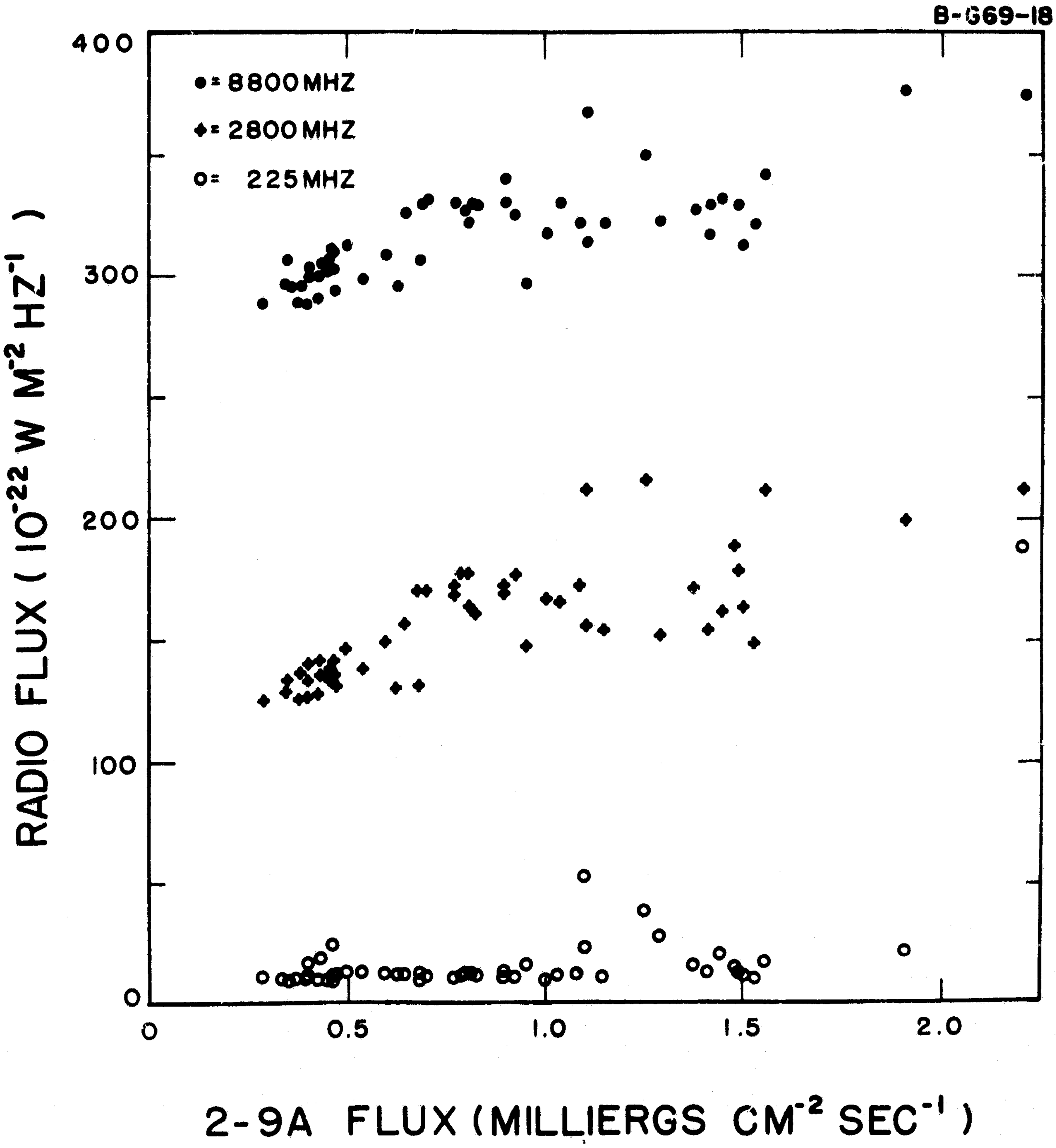
B-G69-18
400
300
200
100
0
0
0.5
1.0
1.5
2.0
● = 8800 MHZ
♦ = 2800 MHZ
o = 225 MHZ
RADIO FLUX (10^{-22} W M^{-2} HZ^{-1})
2-9A FLUX (MILLIERGS CM^{-2} SEC^{-1})

Figure 10

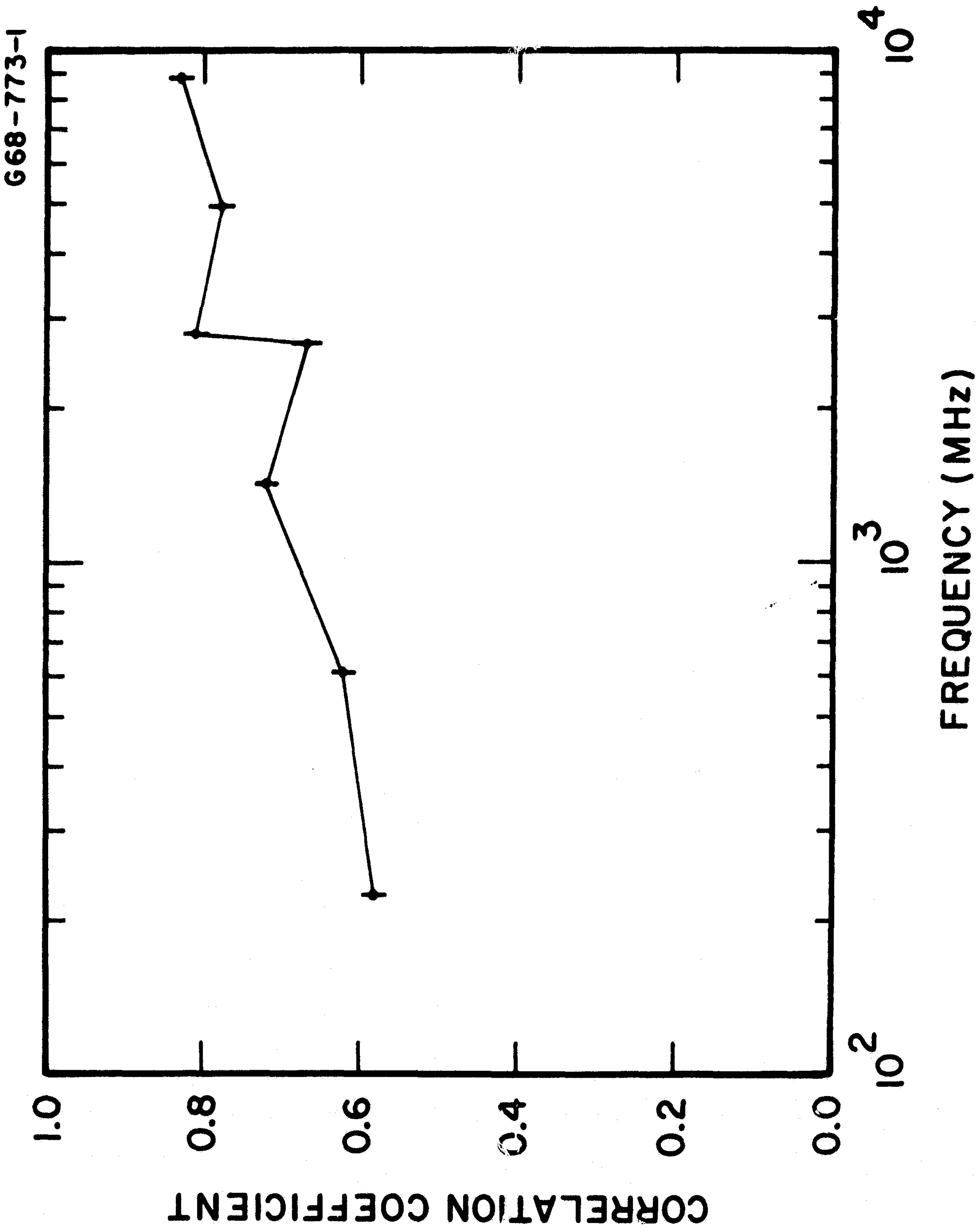
G68-773-1
CORRELATION COEFFICIENT
1.0
0.8
0.6
0.4
0.2
0.0
FREQUENCY (MHz)
10^2
10^3
10^4

Figure 11

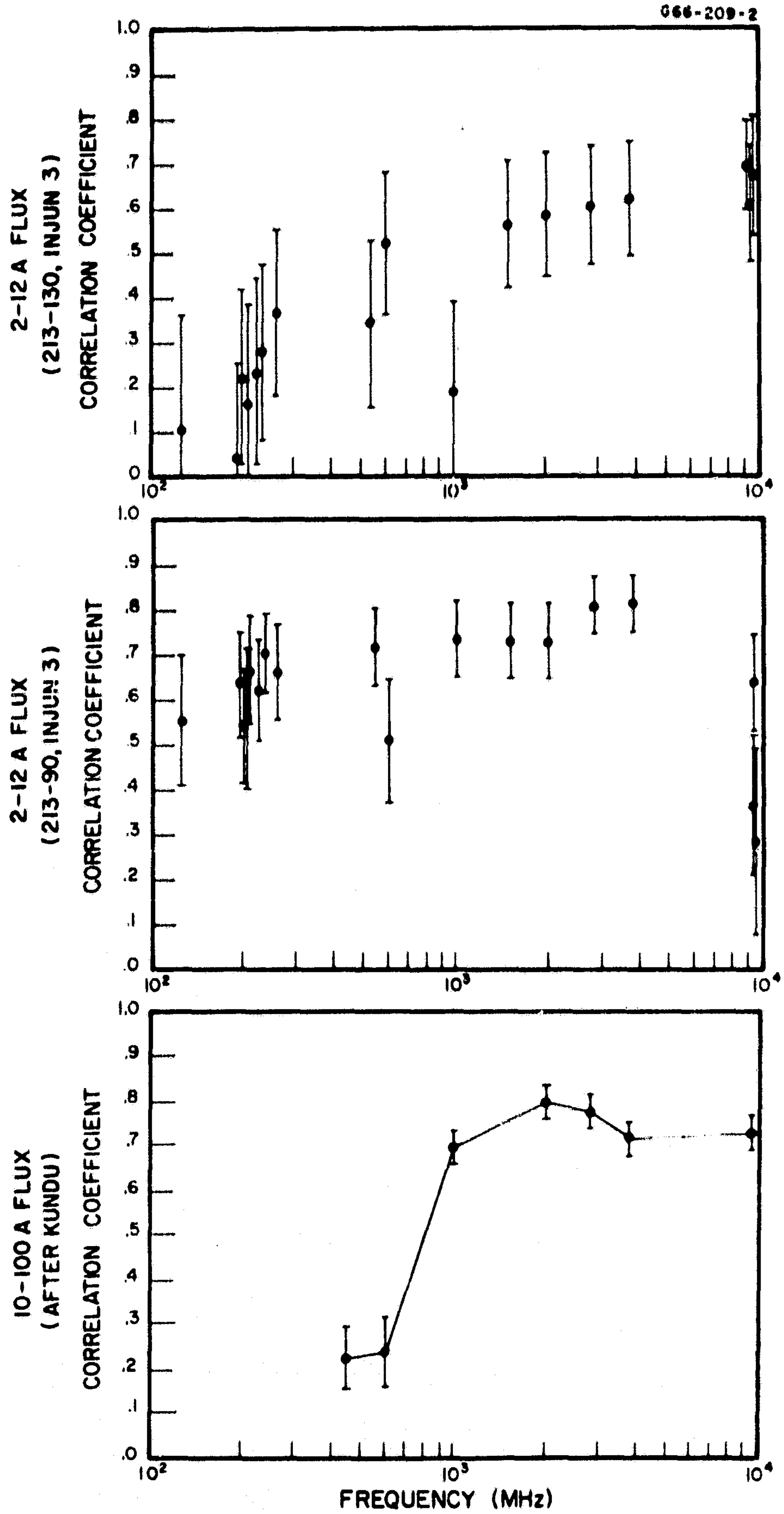
G66-209-2
2-12 A FLUX
(213-130, INJUN 3)
CORRELATION COEFFICIENT
2-12 A FLUX
(213-90, INJUN 3)
CORRELATION COEFFICIENT
10-100 A FLUX
(AFTER KUNDU)
CORRELATION COEFFICIENT
FREQUENCY (MHz)

Figure 12

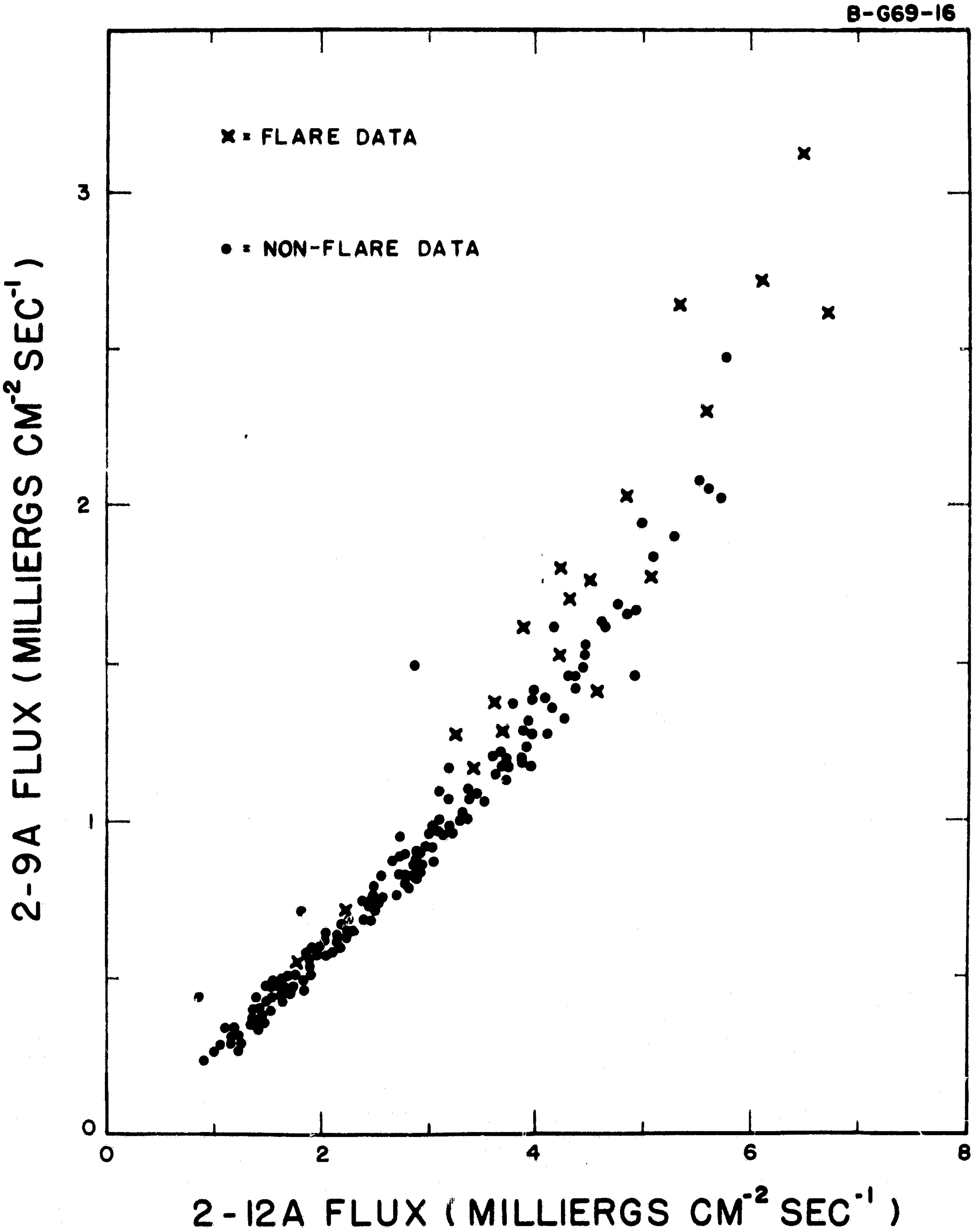
B-G69-16
× = FLARE DATA
● = NON-FLARE DATA
0
1
2
3
0
2
4
6
8
2-9A FLUX (MILLIERGS CM^{-2} SEC^{-1})
2-12A FLUX (MILLIERGS CM^{-2} SEC^{-1})

Figure 13

UNCLASSIFIED

Security Classification

DOCUMENT CONTROL DATA - R&D

(Security classification of title, body of abstract and indexing annotation must be entered when the overall report is classified)

1 ORIGINATING ACTIVITY (Corporate author) Department of Physics and Astronomy The University of Iowa	2a REPORT SECURITY CLASSIFICATION UNCLASSIFIED 2b GROUP

3 REPORT TITLE

The Correlation of Solar Microwave and Soft X-Ray Radiation

1. The Solar Cycle and Slowly Varying Components

4 DESCRIPTIVE NOTES (Type of report and inclusive dates)

Progress Report March 1969

5 AUTHOR(S) (Last name, first name, initial)

Wende, Charles D.

6 REPORT DATE	7a TOTAL NO OF PAGES	7b NO OF REFS
March 1969	40	15

8a CONTRACT OR GRANT NO 1509(06)	9a ORIGINATOR'S REPORT NUMBER(S) U. of Iowa 69-17
b PROJECT NO c d	9b OTHER REPORT NO(S) (Any other numbers that may be assigned this report)

10 AVAILABILITY LIMITATION NOTICES

Distribution of this document is unlimited.

11 SUPPLEMENTARY NOTES	12 SPONSORING MILITARY ACTIVITY
	Office of Naval Research

13 ABSTRACT

[See Page Following]

DD FORM 1 JAN 64 1473

UNCLASSIFIED

Security Classification

UNCLASSIFIED

Security Classification

14 KEY WORDS	LINK A		LINK B		LINK C	
	ROLE	WT	ROLE	WT	ROLE	WT
Sun						
Solar X-Rays						
Solar Radio Noise						
Solar Flares						

INSTRUCTIONS

1. ORIGINATING ACTIVITY: Enter the name and address of the contractor, subcontractor, grantee, Department of Defense activity or other organization *(corporate author)* issuing the report.

2a. REPORT SECURITY CLASSIFICATION: Enter the overall security classification of the report. Indicate whether "Restricted Data" is included. Marking is to be in accordance with appropriate security regulations.

2b. GROUP: Automatic downgrading is specified in DoD Directive 5200.10 and Armed Forces Industrial Manual. Enter the group number. Also, when applicable, show that optional markings have been used for Group 3 and Group 4 as authorized.

3. REPORT TITLE: Enter the complete report title in all capital letters. Titles in all cases should be unclassified. If a meaningful title cannot be selected without classification, show title classification in all capitals in parenthesis immediately following the title.

4. DESCRIPTIVE NOTES: If appropriate, enter the type of report, e.g., interim, progress, summary, annual, or final. Give the inclusive dates when a specific reporting period is covered.

5. AUTHOR(S): Enter the name(s) of author(s) as shown on or in the report. Enter last name, first name, middle initial. If military, show rank and branch of service. The name of the principal author is an absolute minimum requirement.

6. REPORT DATE: Enter the date of the report as day, month, year; or month, year. If more than one date appears on the report, use date of publication.

7a. TOTAL NUMBER OF PAGES: The total page count should follow normal pagination procedures, i.e., enter the number of pages containing information.

7b. NUMBER OF REFERENCES: Enter the total number of references cited in the report.

8a. CONTRACT OR GRANT NUMBER: If appropriate, enter the applicable number of the contract or grant under which the report was written.

8b, 8c, & 8d. PROJECT NUMBER: Enter the appropriate military department identification, such as project number, subproject number, system numbers, task number, etc.

9a. ORIGINATOR'S REPORT NUMBER(S): Enter the official report number by which the document will be identified and controlled by the originating activity. This number must be unique to this report.

9b. OTHER REPORT NUMBER(S): If the report has been assigned any other report numbers *(either by the originator or by the sponsor)*, also enter this number(s).

10. AVAILABILITY/LIMITATION NOTICES: Enter any limitations on further dissemination of the report, other than those imposed by security classification, using standard statements such as:

(1) "Qualified requesters may obtain copies of this report from DDC."

(2) "Foreign announcement and dissemination of this report by DDC is not authorized."

(3) "U. S. Government agencies may obtain copies of this report directly from DDC. Other qualified DDC users shall request through ____________."

(4) "U. S. military agencies may obtain copies of this report directly from DDC. Other qualified users shall request through ____________."

(5) "All distribution of this report is controlled. Qualified DDC users shall request through ____________."

If the report has been furnished to the Office of Technical Services, Department of Commerce, for sale to the public, indicate this fact and enter the price, if known.

11. SUPPLEMENTARY NOTES: Use for additional explanatory notes.

12. SPONSORING MILITARY ACTIVITY: Enter the name of the departmental project office or laboratory sponsoring *(paying for)* the research and development. Include address.

13. ABSTRACT: Enter an abstract giving a brief and factual summary of the document indicative of the report, even though it may also appear elsewhere in the body of the technical report. If additional space is required, a continuation sheet shall be attached.

It is highly desirable that the abstract of classified reports be unclassified. Each paragraph of the abstract shall end with an indication of the military security classification of the information in the paragraph, represented as *(TS)*, *(S)*, *(C)*, or *(U)*.

There is no limitation on the length of the abstract. However, the suggested length is from 150 to 225 words.

14. KEY WORDS: Key words are technically meaningful terms or short phrases that characterize a report and may be used as index entries for cataloging the report. Key words must be selected so that no security classification is required. Identifiers, such as equipment model designation, trade name, military project code name, geographic location, may be used as key words but will be followed by an indication of technical context. The assignment of links, roles, and weights is optional.

ABSTRACT

The integral solar x-ray flux between 2-12 A was measured by the spacecrafts Injun 1, Injun 3, Explorer 33, and Explorer 35. The integral flux between 2-9 A was observed by the Mariner V spacecraft. The data from Injuns 1 and 3 and Explorers 33 and 35, when averaged in monthly intervals, show a long term variation in activity of at least a factor of five between 1961 and 1969. A slowly varying component which tracks the 10 cm radio flux is observed in the x-ray flux. This x-ray flux variation, about a factor of ten, correlates with the appearance of major active regions on the solar disc. This slowly varying component correlates well with radio fluxes at frequencies greater than about 1 GHz and less well with radio fluxes at lower frequencies. The x-ray spectrum, obtained by comparing the 2-9 A flux with the 2-12 A flux, hardens during periods of high solar activity and may harden during flares, but does not soften.